PROCEEDINGS OF SCIENCE

B-meson decay constants with domain-wall light quarks and nonperturbatively tuned relativistic b-quarks

Oliver Witzel*
Center for Computational Science, Boston University,
3 Cummington Mall, Boston, MA 02215, USA
E-mail: owitzel@bu.edu

We report on our progress to obtain the decay constants f_B and f_{B_s} from lattice-QCD simulations on the RBC-UKQCD Collaborations 2+1 flavor domain-wall Iwasaki lattices. Using domain-wall light quarks and relativistic b-quarks we analyze data with several partially quenched light-quark masses at two lattice spacings of $a \approx 0.11$ fm and $a \approx 0.08$ fm.

31st International Symposium on Lattice Field Theory - LATTICE 2013
July 29 - August 3, 2013
Mainz, Germany

*Speaker.

PoS(LATTICE 2013)377

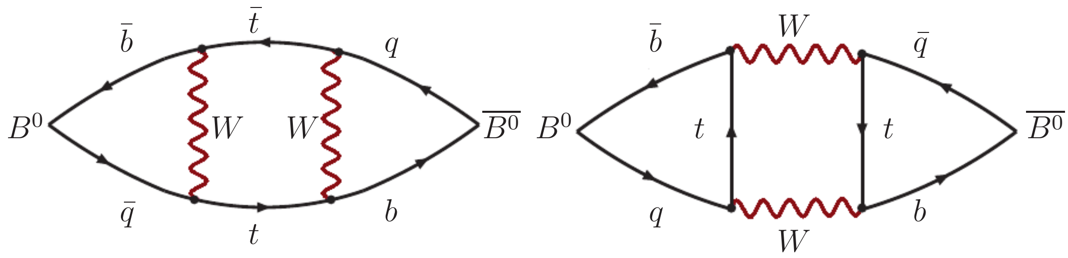

Figure 1: Box-diagrams with top-quarks in the loop are the dominant contributions to neutral B-meson mixing. q denotes either a d- or s-quark.

1. Motivation

B-physics plays a central role in the global efforts to constrain the CKM unitarity triangle. The ratio of neutral B-meson mixing, e.g., is used in the unitarity triangle fits [1–3]. Neutral B-mesons mix with their anti-particle under the exchange of two W-bosons as depicted by the box-diagrams in Fig. 1. There q denotes a light d- or s-quark building either a B- or a B_s-meson, respectively. In the experiments, e.g., BaBar, Belle, CDF or LHCb, B_q-mixing is measured in terms of the oscillation frequencies (mass differences) ΔM_q and in the Standard Model (SM) this process is parameterized by [4]

$$\Delta M_q = \frac{G_F^2 m_W^2}{6\pi^2} \eta_B S_0 M_{B_q} f_{B_q}^2 B_{B_q} |V_{tq}^* V_{tb}|^2, \tag{1.1}$$

where the QCD coefficient η_b [4] and the Inami-Lim function S_0 [5] are computed perturbatively and a nonperturbative computation is needed for the leptonic B_q-meson decay constant f_{B_q} and the bag parameter B_{B_q} in order to extract the CKM matrix elements $V_{tq}^* V_{tb}$. Experimentally ΔM_q is measured to subpercent accuracy [6], whereas the nonpeturbative (lattice) inputs contribute the dominant uncertainty (order few percent). Taking the ratio of neutral B-meson mixing

$$\frac{\Delta M_s}{\Delta M_d} = \frac{M_{B_s}}{M_{B_d}} \xi^2 \frac{|V_{ts}|^2}{|V_{td}|^2}, \tag{1.2}$$

the nonperturbative contribution is contained in the $SU(3)$ breaking ratio

$$\xi = \frac{f_{B_s}\sqrt{B_{B_s}}}{f_{B_d}\sqrt{B_{B_d}}}, \tag{1.3}$$

for which statistical and systematic uncertainties largely cancel [7]. Unfortunately ξ still contributes the largest uncertainty.

We therefore designed this project to compute neutral B-meson mixing matrix elements as well as the leptonic decay constants f_B and f_{B_s}. The decay constants are important to further constrain new physics by allowing an alternative determination of V_{ub} using the measurement of $B \to \tau\nu$ [8–10] or by allowing, e.g., to obtain predictions on rare decays like $B_s \to \mu_+\mu_-$ [11] which promise to be in particular sensitive to new physics.

Computing B-physics quantities on the lattice faces the additional challenge to accommodate an additional scale given by the large b-quark mass. In our project we compute B-physics quantities

Table 1: Lattice simulation parameters used in our B-physics program. The columns list the lattice volume, approximate lattice spacing, light (m_l) and strange (m_h) sea-quark masses, unitary pion mass, and number of configurations and time sources analyzed.

$(L/a)^3 \times (T/a)$	$\approx a$(fm)	am_l	am_h	M_π(MeV)	# configs.	# time sources
$24^3 \times 64$	0.11	0.005	0.040	329	1636	1
$24^3 \times 64$	0.11	0.010	0.040	422	1419	1
$32^3 \times 64$	0.086	0.004	0.030	289	628	2
$32^3 \times 64$	0.086	0.006	0.030	345	889	2
$32^3 \times 64$	0.086	0.008	0.030	394	544	2

using the RBC-UKQCD 2+1 flavor domain-wall Iwasaki gauge field configurations. We simulate the b-quarks with the relativistic heavy quark (RHQ) action and tune the action's parameters non-perturbatively, while domain-wall fermions simulate the light u, d, s-quarks. Thus our project is an independent cross-check to published results by other groups based on 2-flavor [12], 2+1-flavor [13–17] or 2+1+1-flavor [18] gauge-field configurations. In these proceedings we focus on the computation of the B-meson decay constants f_B and f_{B_s}.

2. Computational setup

This computation uses the dynamical 2+1 flavor domain-wall Iwasaki gaugefield configurations generated by the RBC-UKQCD collaboration [19, 20] listed in Tab. 1. We use two coarser, 24^3 ensembles with $a \approx 0.11$fm ($a^{-1} = 1.729$ GeV) and three finer, 32^3 ensembles with $a \approx 0.086$ fm ($a^{-1} = 2.281$ GeV). On the coarser ensembles we place one source per configuration, whereas on the finer ensembles we place two time sources per configuration separated by half the temporal extent of the lattice. For each source we generate six domain-wall [21, 22] propagators with quark masses am_{val}^{24} = 0.005, 0.010, 0.020, 0.030, 0.0343 and 0.040 on the coarser 24^3 ensembles and am_{val}^{32} = 0.004, 0.006, 0.008, 0.025, 0.0272 and 0.030 on the finer 32^3 ensembles. The masses of the three heaviest domain-wall propagators bracket the physical strange quark mass.

We simulate the b-quarks using the the anisotropic Sheikholeslami-Wohlert (clover) action with the relativistic heavy-quark (RHQ) interpretation [23, 24]. The three parameters, m_0a, c_P, ζ, are tuned nonperturbatively using the experimental inputs for the spin-averaged mass $\overline{M}$ and the hyperfine-splitting Δ_M in the B_s-meson system and demanding that the rest mass equals the kinetic mass, i.e., $M_1/M_2 = 1$ [25]. The parameters are tuned by probing seven points of the (m_0a, c_P, ζ) parameter space and then we interpolate to the tuned value by matching to the experimental values.

We use the same seven sets of RHQ parameters in our computation of the decay constants f_B and f_{B_s} because this allows us to cleanly propagate the statistical uncertainty of our tuning procedure to the final results. The decay constants are measured on the lattice by computing the decay amplitude Φ_B which is proportional to the vacuum-to-meson matrix element of the heavy-light axial vector current $\mathscr{A}_\mu = \bar{b}\gamma_5\gamma_\mu q$ and depicted in Fig. 2

$$\langle 0|\mathscr{A}_\mu|B_q(p)\rangle/\sqrt{M_{B_q}} = ip^\mu \Phi^{(0)}_{B_q}/M_{B_q}. \tag{2.1}$$

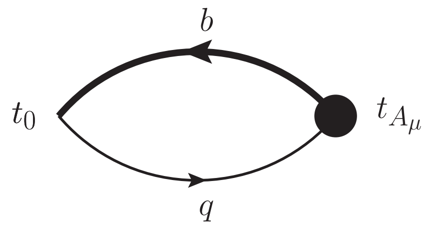

Figure 2: Schematic computation of the decay amplitude Φ_{B_q} with q denoting a d- or s-quark.

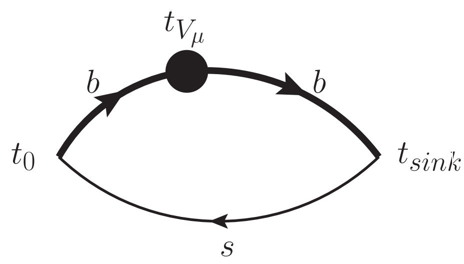

Figure 3: Schematic computation of the flavor-conserving renormalization factor Z_V^{bb} using a s-quark as spectator.

The mass of the B_q-meson is M_{B_q} and p^μ denotes its four momentum. We reduce lattice discretization errors by $O(a)$-improving the axial vector current, $\Phi_{B_q}^{\text{imp}} = \Phi_{B_q}^{(0)} + c_1\Phi_{B_q}^{(1)}$, and compute the coefficient c_1 at 1-loop with mean-field improved lattice perturbation theory [26].

Finally we obtain the decay constant f_{B_q} from $\Phi_{B_q}^{\text{imp}}$ by multiplying the renormalization factor Z_Φ, the lattice spacing and the mass of the B_q-meson

$$f_{B_q} = Z_\Phi \Phi_{B_q}^{\text{imp}} a^{-3/2}/\sqrt{M_{B_q}}. \tag{2.2}$$

For the computation of the renormalization factor Z_Φ we follow the mostly nonperturbative method described in [27] and compute Z_Φ as product of the two nonperturbatively computed, flavor-conserving factors Z_V^{ll} and Z_V^{bb} and a perturbatively computed factor ρ_{bl} which is expected to be close to one and to have a more convergent series expansion in α_s

$$Z_\Phi = \rho_{bl}\sqrt{Z_V^{bb} Z_V^{ll}}. \tag{2.3}$$

The perturbative factor ρ_{bl} is computed at 1-loop with mean-field improved lattice perturbation theory [28] and the RBC-UKQCD collaboration already measured Z_V^{ll} [20]. The factor Z_V^{bb} is determined as part of this project [29].

3. Preliminary results

We determine Z_v^{bb} by measuring the 3-point function describing a B-meson going to a B-meson with the insertion of a vector current between both b-quarks (see Fig. 3)

$$Z_V^{bb} \times \langle B|V^{bb,0}|B\rangle = 2m_B. \tag{3.1}$$

Since Z_V^{bb} does not explicitly depend on the spectator quark, it is advantageous to use a s-quark as spectator because it has smaller statistical uncertainties compared to a lighter quark. For this computation we simulate the b-quarks using a single set of tuned RHQ parameters [25].

We extract Z_V^{bb} from a fit to the plateau of the above defined 3-pt function normalized by the corresponding B_s-meson 2-pt function for each of our five ensembles. Fig. 4 shows example data for Z_V^{bb} on the finer, 32^3 ensemble with light sea-quark mass $a_{32}m_{\text{sea}}^l = 0.006$. The data form a long plateau and the fit interval is chosen such that excited state contamination present in the 2pt-data

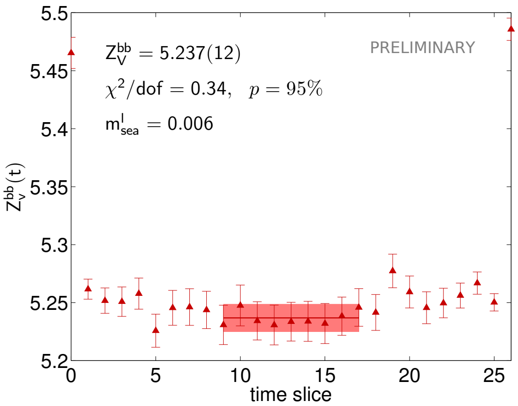

Figure 4: Example plot for the determination of the flavor-conserving renormalization factor Z_V^{bb} on the finer, 32^3 ensemble with $m_{\rm sea}^l = 0.006$.

Table 2: Preliminary results for the nonperturbative determination of the flavor-conserving renormalization factor Z_V^{bb} with statistical errors only. Averaging values at the same lattice spacing we compare to the values obtained from a calculation using 1-loop mean-field improved lattice perturbation theory [26].

$a_{24}m^l_{\rm sea}$	Z_V^{bb}	$a_{32}m^l_{\rm sea}$	Z_V^{bb}
0.005	10.037(34)	0.004	5.270(13)
0.010	10.042(37)	0.006	5.237(12)
		0.008	5.267(15)
Avg.$_{24}$	10.093(25)	Avg.$_{32}$	5.2560(76)
PT$^{\text{1-loop}}_{24}$	10.72	PT$^{\text{1-loop}}_{32}$	5.725

has decayed and is not affecting our signal. Plots for the other ensembles look similar. We list the values for Z_V^{bb} for all our ensembles in Tab. 2. As expected we do not observe a dependence on the sea-quark mass. Furthermore use the results to test the reliability of lattice perturbation theory used for different parts of this project, e.g., the factor ρ_{bl}. We show the results for Z_V^{bb} obtained at 1-loop mean-field improved lattice perturbation theory [26] and compare them to the averages of our nonperturbative determinations. We observe a better-than-expected agreement.

The decay constants and the ratio are obtained by first fitting plateaus of the $O(a)$-improved and renormalized decay amplitudes, $\Phi^{\rm ren}_{B_q} = Z_\Phi \Phi^{\rm imp}_{B_q}$, for all six valence quark masses on our five ensembles. An example for $q = 0.004$ on the 32^3 ensemble with $am^l_{\rm sea} = 0.006$ is given in Fig. 5. We determine f_{B_s} by performing a linear interpolation of the three strange-like data points to the physical value of the strange quark mass. Then we extrapolate the interpolated results on the five ensembles to the continuum with a function that is linear in a^2 (motivated by the leading scaling behavior of the light-quark and gluon actions) and independent of sea-quark mass and obtain $f_{B_s} = 236(5)$ MeV (statistical error only).

The physical value of the decay constant f_B and the ratio f_{B_s}/f_B are obtained from a combined chiral-continuum extrapolation using next-to-leading order SU(2) heavy meson chiral perturbation theory (HMχPT) [30–33]

$$\Phi_B = \Phi_0 \left[1 - \chi^{f_B}_{\rm SU(2)} + c_{\rm sea} m^l_{\rm sea} 2B/(4\pi f)^2 + c_{\rm val} m_{\rm val} 2B/(4\pi f)^2 + c_a a^2/(a^2_{32} 4\pi f)^2\right], \quad (3.2)$$

and

$$\Phi_{B_s}/\Phi_B = R_\Phi \left[1 - \chi^{\rm ratio}_{\rm SU(2)} + c_{\rm sea} m^l_{\rm sea} 2B/(4\pi f)^2 + c_{\rm val} m_{\rm val} 2B/(4\pi f)^2 + c_a a^2/(a^2_{32} 4\pi f)^2\right]. \quad (3.3)$$

The chiral logarithms, $\chi^{f_B}_{\rm SU(2)}$ and $\chi^{\rm ratio}_{\rm SU(2)}$, are nonanalytic functions of the pseudo-Goldstone meson masses, and are given in the appendix of reference [33]. Our preliminary results are shown in Fig. 7. The fits are performed including partially-quenched data on all five sea-quark ensembles, but with valence-quark masses restricted to be below $M_\pi^{\rm val} < 350$ MeV. These extrapolations give

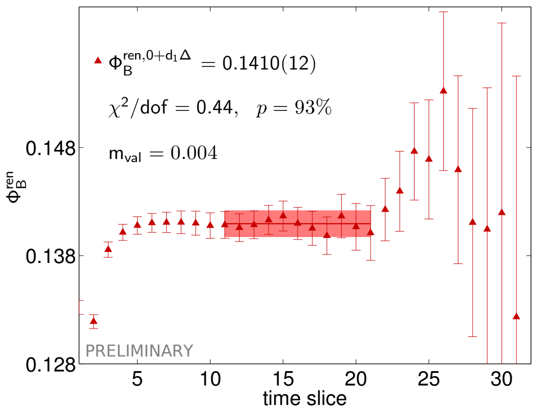

Figure 5: Example plot for the determination of the decay amplitude $\Phi_{B_q}^{ren}$ from a fit to the plateau for light valence quark $q = 0.004$ on the 32^3 ensemble with $am_{\text{sea}}^l = 0.006$.

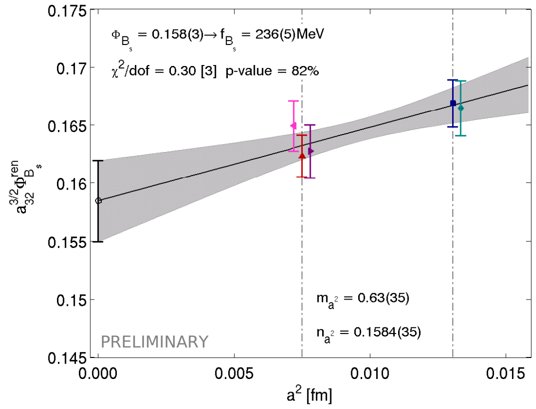

Figure 6: Continuum extrapolation of Φ_{B_s}. The different colored points at each lattice spacing correspond to different sea-quark ensembles, and are horizontally offset for clarity.

us a preliminary value of $f_B = 196(6)$ MeV and a SU(3) breaking ratio of $f_{B_s}/f_{B_q} = 1.21(2)$. Again only statistical uncertainties are quoted. We are finalizing our budget of systematic errors which will also include, e.g., heavy quark discretization errors. All our preliminary results are in agreement with the literature in particular if taking into account that systematic errors will be added.

4. Outlook

We hope to complete and publish our analysis for f_B, f_{B_s} and their ratio f_{B_s}/f_B soon. We anticipate that our largest source of error will be from the chiral-continuum extrapolation. In the future, we will take advantage of the new Möbius domain-wall ensembles generated by the RBC-UKQCD collaboration which feature simulations at the physical pion mass.

Acknowledgments

We thank our colleagues of the RBC and UKQCD collaborations for useful help and discussions. Numerical computations for this work utilized USQCD resources at Fermilab, in part funded by the Office of Science of the U.S. Department of Energy, as well as computers at Brookhaven National Laboratory and Columbia University. O.W. acknowledges support at Boston University by the U.S. DOE grant DE-SC0008814.

References

[1] J. Charles *et al.* (CKMfitter Group), Eur.Phys.J. **C41**, 1 (2005), arXiv:hep-ph/0406184, http://ckmfitter.in2p3.fr/

[2] M. Bona *et al.* (UTfit), JHEP **0507**, 028 (2005), arXiv:hep-ph/0501199, http://utfit.roma1.infn.it/

[3] J. Laiho, E. Lunghi, and R. S. Van de Water, Phys.Rev. **D81**, 034503 (2010), arXiv:0910.2928 [hep-ph], www.latticeaverages.org

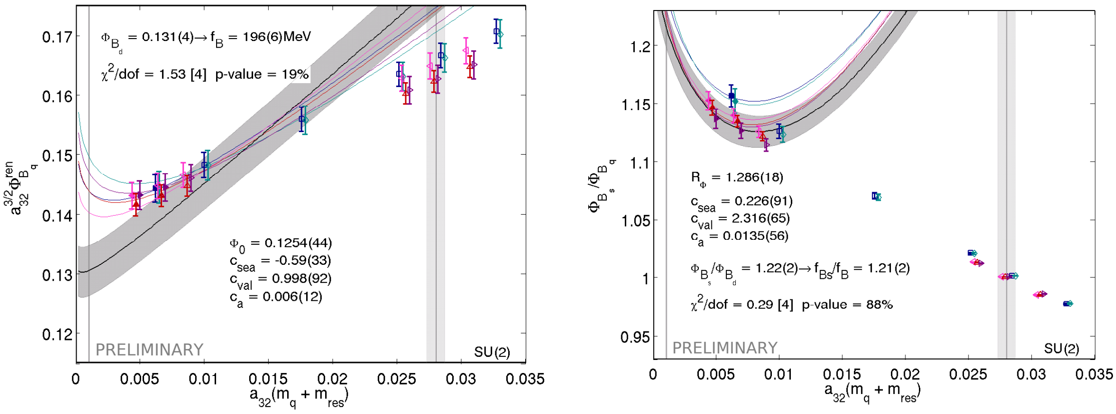

Figure 7: Chiral-continuum extrapolation of Φ_{B_q} (left) and Φ_{B_s}/Φ_{B_q} (right). For better visibility some data points are plotted with a small horizontal offset. Only the filled data points are included in the fit. The vertical gray bands indicate the physical values of the u/d- and s-quark masses [19, 20].

[4] A. J. Buras, M. Jamin, and P. H. Weisz, Nucl. Phys. **B347**, 491 (1990)
[5] T. Inami and C. S. Lim, Prog. Theor. Phys. **65**, 297 (1981)
[6] J. Beringer *et al.* (Particle Data Group), Phys.Rev. **D86**, 010001 (2012)
[7] C. W. Bernard, T. Blum, and A. Soni, Phys.Rev. **D58**, 014501 (1998), arXiv:hep-lat/9801039
[8] E. Lunghi and A. Soni, Phys.Rev.Lett. **104**, 251802 (2010), arXiv:0912.0002 [hep-ph]
[9] M. Bona *et al.* (UTfit), Phys.Lett. **B687**, 61 (2010), arXiv:0908.3470 [hep-ph]
[10] A. Lenz, U. Nierste, and CKMfitter Group, Phys.Rev. **D83**, 036004 (2011), arXiv:1008.1593 [hep-ph]
[11] A. J. Buras *et al.*, JHEP **1307**, 77 (2013), arXiv:1303.3820 [hep-ph]
[12] P. Dimopoulos *et al.* (ETMC), JHEP **1201**, 046 (2012), arXiv:1107.1441 [hep-lat]
[13] E. Gamiz *et al.* (HPQCD), Phys. Rev. **D80**, 014503 (2009), arXiv:0902.1815 [hep-lat]
[14] C. McNeile *et al.* (HPQCD), Phys.Rev. **D85**, 031503 (2012), arXiv:1110.4510 [hep-lat]
[15] H. Na *et al.* (HPQCD), Phys.Rev. **D86**, 034506 (2012), arXiv:1202.4914 [hep-lat]
[16] A. Bazavov *et al.* (Fermilab Lattice-MILC), Phys.Rev. **D85**, 114506 (2012), arXiv:1112.3051 [hep-lat]
[17] A. Bazavov *et al.* (Fermilab Lattice-MILC), Phys.Rev. **D86**, 034503 (2012), arXiv:1205.7013 [hep-lat]
[18] R. Dowdall *et al.* (HPQCD), Phys. Rev. Lett. **110**, 222003 (2013), arXiv:1302.2644 [hep-lat]
[19] C. Allton *et al.* (RBC-UKQCD), Phys. Rev. **D78**, 114509 (2008), arXiv:0804.0473 [hep-lat]
[20] Y. Aoki *et al.* (RBC-UKQCD), Phys.Rev. **D83**, 074508 (2011), arXiv:1011.0892 [hep-lat]
[21] D. B. Kaplan, Phys. Lett. **B288**, 342 (1992), arXiv:hep-lat/9206013
[22] Y. Shamir, Nucl. Phys. **B406**, 90 (1993), arXiv:hep-lat/9303005
[23] N. H. Christ, M. Li, and H.-W. Lin, Phys.Rev. **D76**, 074505 (2007), arXiv:hep-lat/0608006
[24] H.-W. Lin and N. Christ, Phys.Rev. **D76**, 074506 (2007), arXiv:hep-lat/0608005
[25] Y. Aoki *et al.* (RBC-UKQCD), Phys.Rev. **D86**, 116003 (2012), arXiv:1206.2554 [hep-lat]
[26] C. Lehner, PoS **Lattice2012**, 126 (2012), arXiv:1211.4013 [hep-lat], http://physyhcal.lhnr.de
[27] A. X. El-Khadra *et al.*, Phys.Rev. **D64**, 014502 (2001), arXiv:hep-ph/0101023
[28] G. P. Lepage and P. B. Mackenzie, Phys. Rev. **D48**, 2250 (1993), arXiv:hep-lat/9209022
[29] T. Kawanai, R. S. Van de Water, and O. Witzel, PoS **Lattice2012**, 109 (2012), arXiv:1211.0956 [hep-lat]
[30] J. L. Goity, Phys. Rev. **D46**, 3929 (1992), arXiv:hep-ph/9206230
[31] D. Arndt and C. D. Lin, Phys.Rev. **D70**, 014503 (2004), arXiv:hep-lat/0403012
[32] C. Aubin and C. Bernard, Phys. Rev. **D73**, 014515 (2006), arXiv:hep-lat/0510088
[33] C. Albertus *et al.* (RBC-UKQCD), Phys.Rev. **D82**, 014505 (2010), arXiv:1001.2023 [hep-lat]